Di-*tert*-butyl Phosphate Complexes of Cobalt(II) and Zinc(II) as Precursors for Ceramic $M(PO_3)_2$ and $M_2P_2O_7$ Materials: Synthesis, Spectral Characterization, Structural Studies, and Role of Auxiliary Ligands†

Ramaswamy Murugavel,* Malaichamy Sathiyendiran, and Mrinalini G. Walawalkar

Department of Chemistry, Indian Institute of Technology-Bombay, Powai, Mumbai-400 076, India

Received June 6, 2000

Reaction of the metal acetates $M(OAc)_2 \cdot xH_2O$ with di-*tert*-butyl phosphate (dtbp-H) (**3**) in a 4:6 molar ratio in methanol or tetrahydrofuran followed by slow evaporation of the solvent results in the formation of metal phosphate clusters $[M_4(\mu_4\text{-}O)(dtbp)_6]$ (M = Co (**4,** blue); Zn (**5,** colorless)) in nearly quantitative yields. The same reaction, when carried out in the presence of a donor auxiliary ligand such as imidazole (imz) and ethylenediamine (en), results in the formation of octahedral complexes $[M(dtbp)_2(imz)_4]$ (M = Co (**6**); Ni (**7**); Zn (**8**)) and $[Co(dtbp)_2(en)_2]$ (**9**). The tetrameric clusters **4** and **5** could also be converted into mononuclear **6** and **8**, respectively, by treating them with a large excess of imidazole. The use of slightly bulkier auxiliary ligand 3,5-dimethylpyrazole (3,5-dmp) in the reaction between cobalt acetate and **3** results in the isolation of mononuclear tetrahedral complex $[Co(dtbp)_2(3,5\text{-}dmp)_2]$ (**10**) in nearly quantitative yields. Perfectly air- and moisture-stable samples of **4**−**10** were characterized with the aid of analytical, thermoanalytical, and spectroscopic techniques. The molecular structures of the monomeric pale-pink compound **6**, colorless **8**, and deep-blue **10** were further established by single-crystal X-ray diffraction studies. Crystal data for **6**: $C_{28}H_{52}CoN_8O_8P_2$, $a = 8.525(1)$ Å, $b = 9.331(3)$ Å, $c = 12.697(2)$ Å, $\alpha = 86.40(2)°$, $\beta = 88.12(3)°$, $\gamma = 67.12(2)°$, triclinic, $P\bar{1}$, $Z = 1$. Crystal data for **8**: $C_{28}H_{52}N_8O_8P_2Zn$, $a = 8.488(1)$ Å, $b = 9.333(1)$ Å, $c = 12.723(2)$ Å, $\alpha = 86.55(1)°$, $\beta = 88.04(1)°$, $\gamma = 67.42(1)°$, triclinic, $P\bar{1}$, $Z = 1$. Crystal data for **10**: $C_{26}H_{52}CoN_4O_8P_2$, $a = b = 18.114(1)$ Å, $c = 10.862(1)$ Å, tetragonal, $P4_1$, $Z = 4$. The Co^{2+} ion in **6** is octahedrally coordinated by four imidazole nitrogens which occupy the equatorial positions and oxygens of two phosphate anions on the axial coordination sites. The zinc derivative **8** is isostructural to the cobalt derivative **6**. The crystal structure of **10** reveals that the central cobalt atom is tetrahedrally coordinated by two phosphate and two 3,5-dmp ligands. In all structurally characterized monomeric compounds (**6**, **8**, and **10**), the dtbp ligand acts as a monodentate, terminal ligand with free P═O phosphoryl groups. Thermal studies indicate that heating the samples at 171 (for **4**) or 93 °C (for **5**) leads to the loss of twelve equivalents of isobutene gas yielding carbon-free $[M_4(\mu_4\text{−}O)(O_2P(OH)_2)_6]$, which undergoes further condensation by water elimination to yield a material of the composition $Co_4O_{19}P_6$. This sample of **4** when heated above 500 °C contains the crystalline metaphosphate $Co(PO_3)_2$ along with amorphous pyrophosphate $M_2P_2O_7$ in a 2:1 ratio. Similar heat treatment on samples **6**−**8** results in the exclusive formation of the respective metaphosphates $Co(PO_3)_2$, $Ni(PO_3)_2$, and $Zn(PO_3)_2$; the tetrahedral derivative **10** also cleanly converts into $Co(PO_3)_2$ on heating above 600 °C.

Introduction

Metallasilicates and metallaphosphates not only represent the two of the most widely found classes of minerals in nature but also are extensively investigated classes of compounds in view of the complexity of their structures.[1] There have been several efforts in recent years, using different strategies, to synthesize soluble molecular cagelike metallasilicates and phosphates, which can throw some light into the local structures of complex silicate and phosphate materials. In particular, studies on metal containing molecular siloxanes, phosphonates, and phosphates by Roesky (from silanetriols, silyltriamides, alkyl/aryl phosphonic acids),[2] Tilley (from *tert*-butoxy substituted silanols and phosphate esters),[3] Feher (from incompletely condensed silasesquioxanes),[4] Sullivan (from a disiloxanedisilanol),[5] Barron and Mason (from aryl phosphonic acids),[6] and us[7] have opened up new possibilities in assembling inorganic clusters incorporating Si−O−M and P−O−M linkages.

These cluster compounds, apart from modeling the local structures of silicate and phosphate materials, can also be used as *single-source precursors* for the eventual preparation of advanced materials by employing processes such as sol−gel

† Dedicated to Professor Herbert W. Roesky on the occasion of his 65th birthday.

* To whom correspondence should be addressed. Phone: +(22) 576 7163. Fax: +(22) 572 3480. E-mail: rmv@chem.iitb.ernet.in.

(1) (a) Liebau, F. *Structural Chemistry of Silicates*, Springer: New York, 1985. (b) Meier, W. M.; Olson, D. H.; Baerlocher, C. *Atlas of Zeolite Structure Types*, 4th ed.; Elsevier: London, 1996.

(2) (a) Murugavel, R.; Chandrasekhar, V.; Roesky, H. W. *Acc. Chem. Res.* **1996**, *29*, 183. (b) Murugavel, R.; Voigt, A.; Walawalkar, M. G.; Roesky, H. W. *Chem. Rev.* **1996**, *96*, 2205. (c) Walawalkar, M. G.; Roesky, H. W.; Murugavel, R. *Acc. Chem. Res.* **1999**, *32*, 117.

(3) Rulkens, R.; Male, J. L.; Terry, K. W.; Olthof, B.; Khodakov, A.; Bell, A. T.; Iglesia, E.; Tilley, T. D. *Chem. Mater.* **1999**, *11*, 2966, and references therein.

(4) Review: Feher, F. J.; Budzichowski, T. A. *Polyhedron* **1995**, *14*, 3239.

(5) Review: King, L.; Sullivan, A. C. *Coord. Chem. Rev.* **1999**, *189*, 19.

(6) Review: Mason, M. *J. Cluster Sci.* **1998**, *9*, 1.

(7) Murugavel, R. Molecular Titanosiloxanes as Model Compounds and Precursors for Titanosilicate Materials. In *Advances in Metallo-Organic Chemistry*; Bohra, R., Ed.; RBSA Publishers: Jaipur, India, 1999; pp 77−88.

10.1021/ic0006100 CCC: $20.00
Published on Web 12/23/2000

routes.[8] Although the early applications of the sol−gel science were on the use of metal alkoxides as precursors for glasses and similar ceramic materials,[8] later years saw the extension of this process for the preparation of several metal silicate and phosphate assemblies.[9] The most appealing advantage of employing single-source molecular precursor approach is in its ability to provide atomic level control over a material's composition and homogeneity.[10]

After the sol−gel process, a number of research groups have devoted considerable research efforts on the synthesis of single-source precursors which could be conveniently converted into useful materials by simple low-temperature thermolysis. This low-temperature thermolysis pathway, in principle, could be considered as an alternative to the sol−gel process for the preparation of materials. A fair amount of success has already been achieved in using thermolysis route for the preparation of a number of silicate and phosphate ceramics starting from precursors that are made up of silanols and phosphorus acids with *tert*-butoxy groups. The use of *tert*-butoxy group substituted silanol [(*t*-BuO)$_3$SiOH] in the preparation of siloxanes of titanium or zirconium was first studied by Abe in 1970.[11] The advantage of *tert*-butoxy groups undergoing facile isobutene gas elimination, at temperatures often lower than 150 °C, has been more recently utilized by Tilley and co-workers.[12−14] Using some simple and elegant synthetic methodologies and starting from [(*t*-BuO)$_3$SiOH] (**1**),[15] [(*t*-BuO)$_2$Si(OH)$_2$] (**2**),[16] and [(*t*-BuO)$_2$P(O)OH] (**3**),[17] these authors have described the preparation of a multitude of siloxane and phosphorus clusters which decompose to the respective ceramic materials. In almost all cases, under thermolysis conditions, the carbon content of the precursor molecule is completely lost below 200 °C, while the remaining hydrogen content is lost as water approximately between 200 and 500 °C.

Scheme 1

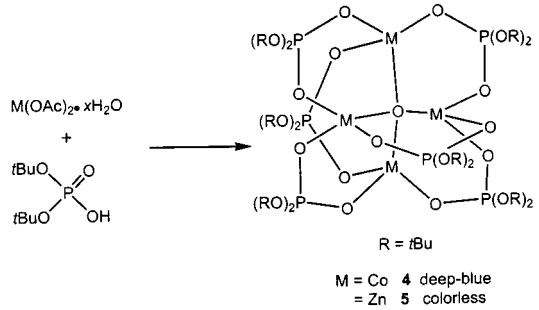

However, all the metal precursor complexes obtained to date from ligands **1**−**3** have been synthesized by employing a metal alkyl, alkoxide, or amide (e.g. $ZnMe_2$, $[Cu(O\text{-}t\text{-}Bu)]_4$, $[Zr(NEt_2)_4]$ as the metal source. Apart from the fact that these starting materials are less readily available, their manipulation also requires anaerobic conditions. It has also been observed that some of the precursor complexes obtained from these starting materials also decompose on exposure to moisture and air. Hence, the use of simpler and cheaper starting materials such as transition metal halides or carboxylates, to achieve ceramic materials is highly desired.

Continuing our recent research efforts on the metal phosphate chemistry, we wish to describe herein (a) the synthesis of polyhedral clusters $[M_4(\mu_4\text{−}O)(dtbp)_6]$ (M = Co or Zn) starting from commercially available metal acetates, (b) the modulation of structural types of the resultant phosphates in the presence of an auxiliary ligand such as imidazole, ethylenediamine, or 3,5-dimethylpyrazole, (c) spectral and structural characterization of the products, and (d) the conversion of the precursor complexes to the desired ceramic meta- and pyrophosphates.

Results and Discussion

Synthesis of $[M_4(\mu_4\text{-}O)(dtbp)_6]$ (M = Co 4; Zn 5). During the attempts to prepare molecular metal phosphates of the formula $[M(dtbp)_2]$ from the reactions between the respective $M(OAc)_2$ and dtbp-H (**3**), the phosphate clusters $[M_4(\mu_4\text{−}O)(dtbp)_6]$ (M = Co (**4**); Zn (**5**)) were obtained as the products. Variations in terms of reaction conditions or the choice of the reaction medium did not alter the nature of the final product obtained in these reactions. Quantitative amounts of the tetrahedral clusters, however, can be obtained as the only products by choosing a 4:6 ratio of the metal acetate and ligand in an optimized reaction medium of commercial grade methanol (Scheme 1). While the zincophosphate cluster **5** precipitates as a white solid (which can be easily separated by simple filtration), the deep-blue colored cobalt phosphate **4** was obtained as microcrystals by standing the reaction mixture for several days (vide infra). The products obtained in both the cases, after vacuum-drying to remove any occluded acetic acid, were found to be analytically and spectroscopically pure and did not warrant any further purification for subsequent studies. They were also found to be very stable in the presence of moist air and hence no precautions were taken in handling these samples. Although the cobalt phosphate **4** is deep-blue in the solid state, on dissolution in methanol, the color of the solution becomes pale-pink. From this pale-pink solution deep-blue microcrystals are formed along the walls of the flask during slow evaporation of the solvent methanol. This observation suggests that in methanol solution the cobalt atoms are additionally coordinated by solvent molecules to form an octahedral environment; however in the solid state the cobalt centers prefer a tetrahedral environment.

(8) (a) Brinker, C. J.; Scherer, G. W. *Sol−Gel Science*; Academic Press: Boston, 1990. (b) *Sol- Gel Technology for Thin Films, Fibres, Preforms, Electronics, and Speciality Shapes*; Klein, L. C., Ed.: Noyes Publishers, Parkridge, NJ, 1988. (c) Corriu, R. J. P.; Leclercq, D. *Angew. Chem., Int. Ed. Engl.* **1996**, *35*, 1421. (d) Mehrotra, R. C. *J. Non-Cryst. Solids* **1996**, *121*, 1. (e) Bradley, D. C.; Mehrotra, R. C.; Gaur, D. P. *Metal Alkoxides*; Academic Press: London, 1978. (f) Mehrotra, R. C. *Struct. Bonding* **1992**, *77*, 1.

(9) (a) Che, M.; Cheng, Z. X.; Louis, C. *J. Am. Chem. Soc.* **1995**, *117*, 208. (b) Mostafa, M. R.; Youssef, A. M. *Mater. Lett.* **1998**, *34*, 405. (c) Harmer, M. A.; Vega, A. J.; Flippen, R. B. *Chem. Mater.* **1994**, *6*, 1903.

(10) (a) Williams, A. G.; Interrante, L. V. In *Better Ceramics Through Chemistry*; Brinker, C. J., Clark, D. E., Ulrich, D. R., Eds.; Materials Research Society Symposia Proceedings, Vol. 32; North-Holland Publishers: New York, 1984. (b) Chandler, C. D.; Roger, C.; Hampden-Smith, M. J. *Chem. Rev.* **1993**, *93*, 1205.

(11) (a) Abe, Y.; Kijima, I. *Bull. Chem. Soc. Jpn.* **1970**, *43*, 466. (b) Abe, Y.; Hayama, K.; Kijima, I. *Bull. Chem. Soc. Jpn.* **1972**, *45*, 1258.

(12) (a) Terry, K. W.; Tilley, T. D. *Chem. Mater.* **1991**, *3*, 1001. (b) Terry, K. W.; Lugmair, C. G.; Tilley, T. D. *J. Am. Chem. Soc.* **1997**, *119*, 9745. (c) Terry, K. W.; Gantzel, P. K.; Tilley, T. D. *Chem. Mater.* **1992**, *4*, 1290. (d) Terry, K. W.; Gantzel, P. K. Tilley, T. D. *Inorg. Chem.* **1993**, *32*, 5402. (e) Terry, K. W.; Lugmair, C. G.; Gantzel, P. K.; Tilley, T. D. *Chem. Mater.* **1996**, *8*, 274. (f) Su, K.; Tilley, T. D. *Chem. Mater*. **1997**, *9*, 588. (g) Su, K.; Tilley, T. D.; Sailor, M. J. *J. Am. Chem. Soc.* **1996**, *118*, 3459 (h) Terry, K. W.; Su, K.; Tilley, T. D.; Rheingold, A. L. *Polyhedron* **1998**, *17*, 891. (i) Rulkens, R.; Tilley, T. D. *J. Am. Chem. Soc.* **1998**, *120*, 9959.

(13) (a) Lugmair, C. G.; Tilley, T. D. *Inorg. Chem.* **1998**, *37*, 1821. (b) Lugmair, C. G.; Tilley, T. D.; Rheingold, A. L. *Chem. Mater.* **1999**, *11*, 1615.

(14) Lugmair, C. G.; Tilley, T. D.; Rheingold, A. L. *Chem. Mater.* **1997**, *9*, 339.

(15) Abe, Y.; Kijima, I. *Bull. Chem. Soc. Jpn.* **1969**, *42*, 1118.

(16) Miner, C. S., Jr.; Bryan, L. A.; Holysz, R. P.; Pedlow, G. W., Jr. *Ind. Eng. Chem.* **1947**, *39*, 1368.

(17) Zwierzak, A.; Kluba, M. *Tetrahedron* **1971**, *27*, 3163.

Table 1. Selected Physical, Analytical and Spectroscopic Data for **4**−**10**

		elem anal [found (calcd)]			IR spectral data		UV−vis spectral data[a]
compd	% yield	C	H	N	ν(P=O) (cm^{-1})	ν(P−O−M) (cm^{-1})	λ_{max} (cm^{-1})
4	93	37.8 (38.3)	7.4 (7.2)		1183	1078; 1003	19 600, 34 600
5	83	37.7 (37.6)	7.0 (7.1)		1191	1089; 1001	
6	85	44.2 (44.9)	7.0 (7.0)	15.0 (15.0)	1216	1071; 985	17 670, 18 940, 33 780
7	86	45.7 (44.9)	7.0 (7.0)	14.6 (14.9)	1213	1070; 976	16 080, 26 670, 33 900
8	71	44.6 (44.5)	7.2 (6.9)	14.7 (14.8)	1211	1070; 978	34 720
9	70	39.9 (40.1)	9.4 (9.1)	9.5 (9.3)	1189	1071; 979	21 370, 29 410, 34 840
10	79	46.7 (46.6)	8.2 (7.8)	8.2(8.4)	1182	1086; 977	16 640, 17 450, 34 480

[a] In MeOH.

The solution and solid state diffuse reflectance visible spectral data also lend evidence to this supposition.

The zincophosphate cluster **5** has been also described recently by Tilley and co-workers, who initially obtained this product in a reaction between $ZnMe_2$ and **3** in the presence of adventitious water.[14] By deliberate addition of water to the reaction medium and also altering the stoichiometry of the reactants, these authors have obtained **5** in about 61% yield from a pentane solution. Apart from an increased yield obtained by us, quite surprisingly, a few essential differences have been observed in the properties of **5** depending on the synthetic methodology used for its preparation. For example, while we observe that a pure dry sample of **5** prepared from $Zn(OAc)_2$ is practically insoluble in hydrocarbons and is only partially soluble in solvents such as toluene and THF, the sample prepared by Tilley using $ZnMe_2$ shows a greater solubility even in pentane. However, the most striking difference between the samples prepared by these two different routes is evident from their thermal studies (vide infra).

Spectra and Structures of 4 and 5. Surprisingly, despite the presence of several bulky *tert*-butoxy groups, cluster **4** is insoluble in most organic solvents and also in water precluding the characterization of the complex in solution.[18] Hence, phosphate **4** has been characterized in the solid state with the aid of analytical data, mass, IR and visible spectral studies, and thermal analysis. Key spectral data for all the compounds reported in this study are listed in Table 1.

In the EI mass spectrum of the sample, the heaviest peak obtained at m/z 1506 (55%) corresponds to the molecular ion $[Co_4(\mu_4\text{−}O)(dtbp)_6]^+$. Expectedly, desorption chemical ionization (DCI) mass spectrum of **4** (in the presence of NH_3) yields peaks due to $[M + H]^+$ and $[M + NH_4]^+$ ions (M = molecular ion) with 40 and 35% abundance, respectively. The deep-blue color of the compound **4** and its visible spectrum both in solution and solid state clearly indicate that the Co^{2+} ions in **4** are in a tetrahedral environment (Table 1). A strong IR absorption observed at 1078 cm^{-1} for **4** is characteristic of the M−O−P absorption, as has been observed in the case of several metallaphosphates and phosphonates in the range 1000−1100 cm^{-1}.[19] Further, the spectra are devoid of any absorption in the region 3000−3500 cm^{-1}, indicating complete reaction of P−OH with metal acetates. The UV−vis spectral maxima in methanol for this pink colored complex are observed around 19 600 and 34 600 cm^{-1}. While the 19 610 cm^{-1} absorption is assignable to the (ν_3) $^4T_{1g}(F) \rightarrow {}^4T_{1g}(P)$ transition of the octahedral cobalt (II) complex, the sharp band at 34 600 cm^{-1} could be attributed to the LMCT in the ultraviolet region. The DR UV spectrum of compound **4** revealed the characteristic complex absorption associated with tetrahedrally coordinated Co(II).

Although, thus far, it has not been possible to grow single crystals of **4** suitable for X-ray diffraction studies, the analytical data, and EI and DCI mass spectral data clearly indicate that the cobalt cluster has the structure of basic zinc acetate $[Zn_4(\mu_4\text{-}O)(OAc)_6]$,[20] zincophosphate $[Zn_4(\mu_4\text{-}O)(dtbp)_6]$ (**5**),[14] and other carboxylates and dialkyldithiophosphates of zinc.[21] While the quadruply oxygen bridged tetrahedral clusters are common in the case of compounds of zinc,[14,20,21] there are only a few examples of well-characterized $[Co_4(\mu_4\text{-}O)L_6]$ type of clusters described in the literature.[22] In fact compound **4** represents the first well-characterized tetrahedral cluster of Co containing phosphate, phosphonate, or phosphinate type of ligand.

Solid-State Thermolysis of 4. Heating a sample of **4** in a glass capillary in a melting point apparatus showed a number of changes in the physical appearance of the sample with some gas evolution. This prompted a detailed investigation of the thermal decomposition behavior of solid **4.** The TGA curve of **4** (Figure 1) shows the onset of a large weight loss at 144 °C, which loses 45 wt % of the sample before 195 °C. An endotherm corresponding to this weight loss is observed at 171 °C in the DTA curve. Heating the sample beyond 195 °C results in a further slow weight loss of about 7% before the temperature reaches 500 °C. From this point onward the TGA curve shows almost a straight line up to 1000 °C, indicating no further weight loss.

The changes observed in the TGA and DTA of compound **4** can be understood by considering a sequence of events shown in Figure 2. The first weight loss corresponding to the loss of ∼45% of the original material can readily be interpreted as the loss of 12 equiv of isobutene gas from the 6 dtbp ligands leaving 12 P−O−H moieties (theoretical weight loss 44.6%). Due to the low kinetic stability of the $-P(OH)_2$ units, a further weight

(18) However, the sample is soluble to a very less extent in toluene mixed with small amounts of methanol.

(19) Walawalkar, M. G.; Murugavel, R.; Roesky, H. W.; Schmidt, H.-G. *Inorg. Chem.* **1997**, *36*, 4202.

(20) (a) Lee, J. D. *Concise Inorganic Chemisrty*, 4th ed.; Chapman & Hall: London, 1991; Chapter 28. (b) Kunkey, H.; Vogler, A. *J. Chem. Soc., Chem. Commun.* **1990**, 1204. (c) Bertoncello, R.; Bettinelli, M.; Casarin, M.; Gulino, A.; Tondello, E.; Vittadini, A. *Inorg. Chem.* **1992**, *31*, 1558.

(21) Clusters with $[Zn_4O]^{6+}$ core: (a) Koyama, H.; Saito, Y. *Bull. Chem. Soc. Jpn.* **1954**, *27*, 112. (b) Cen, W.; Haller, K. J.; Fehliner, T. P. *Inorg. Chem.* **1991**, *30*, 3120. (c) Belforte, A.; Calderazzo, F.; Englert, U.; Strahle, J. *Inorg. Chem.* **1991**, *30*, 3778. (d) Konno, T.; Nagashio, T.; Okamoto, K.; Hidaka, J. *Inorg. Chem.* **1992**, *31*, 1160. (e) Okamoto, K.; Watanable, Y.; Konno, T.; Hidaka, J. *Bull. Chem. Soc. Jpn.* **1992**, *65*, 3015. (f) Lee, C. F.; Chin, K. F.; Peng, S. M.; Che, C. M. *J. Chem. Soc., Dalton Trans.* **1993**, 467. (g) Burn, A. J.; Joyner, R. W.; Meehan, P.; Parker, K. M. A. *J. Chem. Soc., Chem. Commun.* **1986**, 982. (h) Burn, A. J.; Dewan, S. K.; Gosney, I.; Tan, P. S. G. *J. Chem. Soc., Perkin. Trans.* **1990**, 1311.

(22) To our knowledge there are only a few examples of clusters with a $[Co_4O]^{6+}$ core; see: (a) Peng, S. M.; Lin, Y. N. *Acta Crystallogr., Sect. C* **1986**, *42*, 1725. (b) Schmid, R.; Mosser, A.; Galy, J. *Inorg. Chim. Acta.* **1991**, *179*, 167. (c) Jaitner, P.; Ricker, C.; Wurst, K. *Chem. Commun.* **1997**, *1245*. (d) Okamato, K.; Konno, T.; Hidaka, J. *J. Chem. Soc., Dalton Trans.* **1994**, 533. (e) Ehlert, M. K.; Rettig. S. J.; Storr, A.; Thompson, R. C.; Trotter, J. *Acta Crystallogr., Sect. C* **1994**, *50*, 1023. (f) Cotton, F. A.; Daniels, L. M.; Falvello, L. R.; Matonic, J. H.; Murillo, C. A.; Wang, X.; Zhou, H. *Inorg. Chim. Acta* **1997**, *266*, 91.

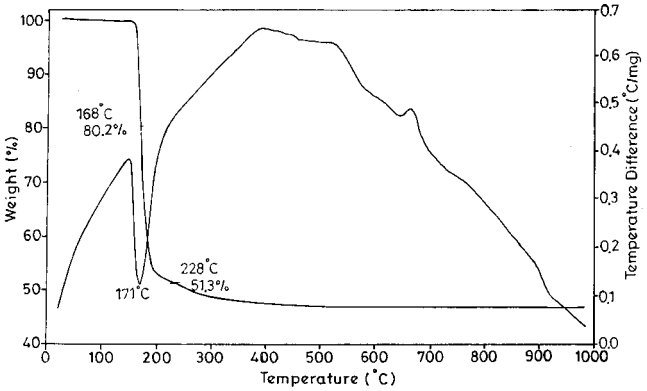

Figure 1. TGA and DTA traces of $[Co_4(\mu_4\text{–}O)(dtbp)_6]$ (**4**).

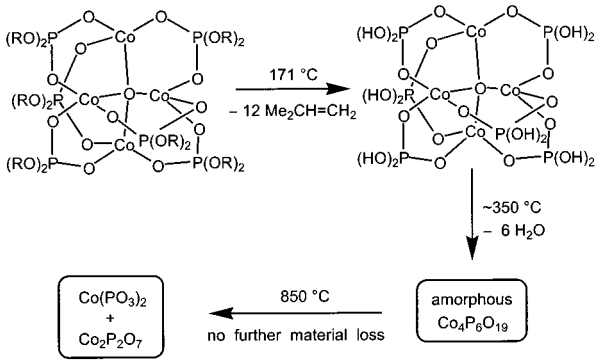

Figure 2. Sugested thermal decomposition pathway for $[Co_4(\mu_4\text{–}O)(dtbp)_6]$ (**4**).

loss results at ~350 °C by the elimination of 6 equiv of H_2O molecules resulting in a ceramic material of the composition $Co_4P_6O_{19}$. There was no formation of P_2O_5 in the process, and the ceramic material obtained at the end of the thermolysis at 1000 °C accounts for the presence of only cobalt meta- and pyrophosphates, $Co(PO_3)_2$ and $Co_2P_2O_7$. The XRD pattern of the independently calcined samples at 850 °C showed the presence of $Co(PO_3)_2$ in the material.[23] The broad features of the XRD spectrum clearly indicates the presence of an amorphous component (presumably $Co_2P_2O_7$) along with the metaphosphate.[24]

Solid-State Thermolysis of 5. Although the thermolysis of **5** has already been carried out by Tilley et al., due to the minor changes in the properties of the compound described vide supra, the compound prepared through the acetate route in the present study was again subjected to a thermolysis study. Interestingly, the TGA studies reveal that there is a large difference in the temperature at which the *tert*-butoxy groups decompose to eliminate isobutene gas. For example, while Tilley et al. report 134 °C as the onset of the decomposition of the *tert*-butoxy groups of sample **5** prepared from $ZnMe_2$ in the organic medium, the decomposition starts at 79 °C in the present case (see Supporting Information). Thus, while the endotherm corresponding to the loss of *tert*-butoxy groups occur at 93 °C in the present case, the corresponding endotherm for the sample prepared from $ZnMe_2$ occurs at 139 °C.[14] The observed difference in the temperature of the isobutene evolution (approximately 45°) could only be attributed to the nature of the medium of preparation of the samples.[25]

Scheme 2

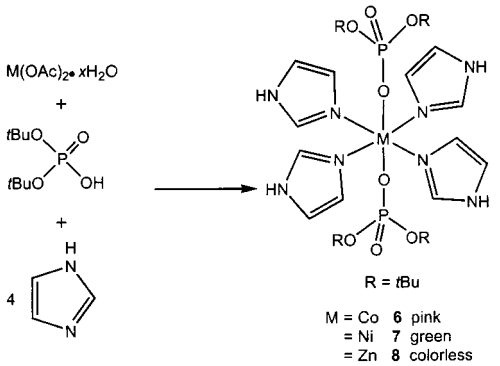

Imidazole as Auxiliary Ligand. While the direct reaction between the metal acetates and dtbp-H leads to the tetrahedral clusters **4** and **5** with a metal-to-dtbp ratio of 4:6, it was anticipated that it should be possible to obtain different types of clusters/mononuclear complexes with a different metal to phosphate ligand ratio if the reactions are carried out in the presence of donor ligands. Hence, to probe into the role of amino auxiliary ligands,[26] the above reactions have been repeated in the presence of donor amines such as imidazole, ethylenediamine, and 3,5-dimethylpyrazole.

Quite interestingly, the reactions of $M(OAc)_2.xH_2O$ with dtbp-H in the presence four or more equivalents of imidazole leads to the isolation of the products with the empirical formula $[M(dtbp)_2(imz)_4]$ (M = Co 6; Ni **7**; Zn **8**) (Scheme 2). The elemental analysis, IR, and UV−Vis data (Table 1) reveal that in the resultant compounds the metal ions are coordinated to four imidazole and two dtbp ligands. The IR spectrum of **6** in KBr exhibits strong absorptions at 1216 and 1071 cm^{-1}, indicating the presence of phosphoryl oxygen atoms and P−O−M linkages, respectively (Table 1). Nonobservance of any large shift in the absorbance of the phosphoryl group (ν(P═O)) for the free ligand 1230 cm^{-1}) suggests that the P═O group does not take part in coordination to the metal.

Compound **6** is pink in color both as solid and methanol solution, indicating an octahedral arrangement around the metal ion both in solid state and in solution. Three absorption maxima were observed in the visible spectrum for **6** at 17 670, 18 940, and 33 780 cm^{-1}. The two former absorptions are assigned as (ν_3) $^4T_{1g}(F) \rightarrow {}^4T_{1g}(P)$ transitions of the octahedral Co(II).[27,28] Similarly the UV−vis spectra of the green colored nickel complex **7** shows two bands at 16 080 ($^3A_{2g}(F) \rightarrow {}^3T_{1g}(F)$) and 26 670 ($^3A_{2g}(F) \rightarrow {}^3T_{1g}(P)$), indicating once again a octahedral coordination geometry around the Ni(II) metal ion.[27,29] The NMR spectrum of the diamagnetic compound **8** shows resonances at δ 7.0 and 7.7 ppm in a 2:1 ratio, which could be assigned to the protons of the imidazole heterocycle. Expectedly, the CH_3 protons of the *tert*-butoxy groups resonate as a singlet at 1.3 ppm.

Molecular Structures of 6 and 8. To further probe into the molecular structures of the $[M(dtbp)_2(imz)_4]$ complexes, single-crystal X-ray diffraction studies were carried out for isomorphic

(23) (a) PDF# 190351, 1.54184 (b) PDF# 271120, 1.54184. *NBS Monogr. (U.S.)* 1976, *25*, 13, 23.

(24) Although we are not able to pick up the XRD pattern of the pyrophosphate $Co_2P_2O_7$ from the samples prepared under the conditions described, it is reasonable to assume that the mixture contains both $Co(PO_3)_2$ and $Co_2P_2O_7$ based on the detailed decomposition studies carried out by Tilley[14] for the analogous zinc derivative **5**.

(25) Repeating the TGA and DTA of **5** from the sample prepared from different batches produce the same result.

(26) For the role of auxiliary amine ligands in metal phosphonate chemistry, see: (a) Chandrasekhar, V.; Kingsley, S. *Angew. Chem., Int. Ed. Engl.* 2000, *39*, 2320.

(27) Lever, A. B. P. *Inorganic Electronic Spectroscopy*, 2nd ed.; Elsevier: Amsterdam, 1984.

(28) Verberckmoes, A. A.; Weckhuysen B. M.; Schoonheydt, R. A. *Microporous Mesoporous Mater.* **1998**, *22*, 165.

(29) Mathews, R. W.; Walton, R. A. *Inorg. Chem.* **1971**, *10*, 1433.

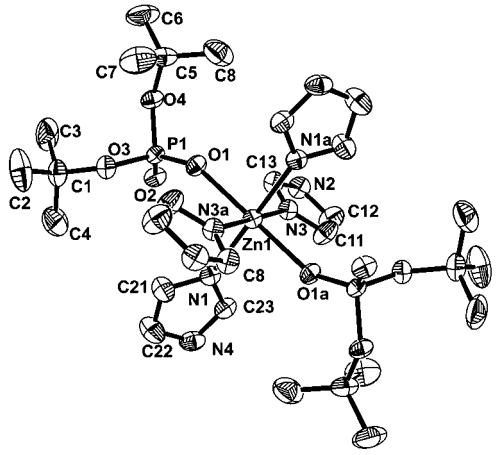

Figure 3. Thermal ellipsoid plot of $[Zn(dtbp)_2(imz)_4]$ (8) at 50% probability level; Compound **6** is isomorphous.

Table 2. Selected Bond Lengths (Å) and Angles (deg) for **6** and **8**

	6	**8**
M−O(1)	2.135(3)	2.181(2)
M−N(1)	2.102(4)	2.102(2)
M−N(3)	2.178(4)	2.208(2)
P(1)−O(1)	1.486(3)	1.478(2)
P(1)−O(2)	1.498(3)	1.493(2)
P(1)−O(3)	1.583(3)	1.591(2)
P(1)−O(4)	1.574(4)	1.589(2)
O(3)−C(1)	1.476(6)	1.459(4)
O(4)−C(5)	1.479(6)	1.460(4)
N(1)−M−N(1a)	180.0(2)	180.0(1)
O(1)−M−O(1a)	180.0(2)	180.0(1)
N(1)−M−O(1)	91.1(1)	91.6(1)
N(1a)−M−O(1)	88.9(1)	88.4(1)
N(1)−M−N(3)	89.6(2)	90.4(1)
O(1)−M−N(3)	92.0(1)	91.7(1)
N(1)−M−N(3a)	90.4(2)	89.6(1)
O(1)−M−N(3a)	88.0(1)	88.4(1)
N(3)−M−N(3a)	180.0(3)	180.0(2)
O(1)−P(1)−O(2)	119.3(2)	119.5(1)
O(1)−P(1)−O(4)	112.0(2)	111.5(1)
O(2)−P(1)−O(4)	103.1(2)	103.3(1)
O(1)−P(1)−O(3)	105.1(2)	105.0(1)
O(2)−P(1)−O(3)	111.1(2)	111.2(1)
O(4)−P(1)−O(3)	105.5(2)	105.7(1)
P(1)−O(1)−M	147.9(2)	147.1(1)
C(1)−O(3)−P(1)	127.8(3)	127.8(2)
C(5)−O(4)−P(1)	128.1(3)	128.0(2)

compounds **6** and **8**. The elemental analysis, IR and mass spectra of the nickel compound **7** reveal that its structure is also isomorphous to compounds **6** and **8**.

A perspective view of the thermal ellipsoid plot of **8** with atom labeling scheme is shown in Figure 3. Selected bond lengths and angles for both **6** and **8** are listed in Table 2. The single-crystal X-ray structure of $[Zn(dtbp)_2(imz)_4]$ depicted in Figure 3 reveals an octahedrally coordinated Zn(II) ion surrounded by four imidazole molecules in the equatorial positions and two dtbp ligands in the axial positions. The dtbp ligands bind the metal in a unidentate fashion and the P═O functionality is not involved in coordination to the metal. The phosphoryl oxygen, however, forms intermolecular hydrogen bonds to the imidazole N−H groups of the neighboring molecules to result in a tubular structure in the solid state (Figure 4). Table 2 lists selected bond lengths and angles for the imidazole derivatives **6** and **8**. There are no larger variations in the metric parameters of **6** and **8**. The M−O distances (2.135(3) and 2.181(2) Å) are slightly longer than those observed for **10** (vide infra). The cis and trans L−M−L angles around the metal do not vary much from their ideal values. While the cis angles in **6** are in the range 88.0−92.0°, the observed trans angles are 180°. The P−O−M angles (147.9(2)° for **6**; 147.1° for **8**) are more linear than the corresponding values observed for **10** (∼141°).

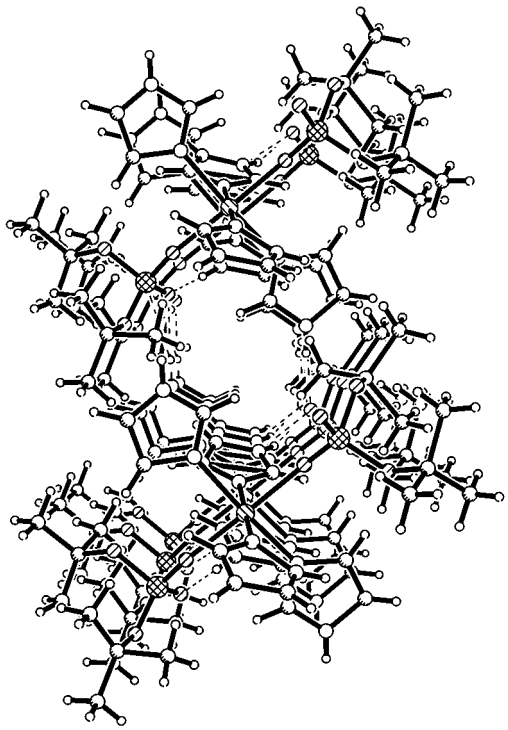

Figure 4. Solid-state packing of molecules of $[Co(dtbp)_2(imz)_4]$ (**6**) in crystal showing the N−H···O═P hydrogen bonds which are responsible for the formation of a channel structure.

Thermal Studies on 6−8. Thermolysis studies of compounds **6**−**8** would prove more interesting due to the 1:2 stoichiometry of metal to phosphate ligand in these complexes (unlike the 4:6 stoichiometry in the cluster compounds **4** and **5**). Preliminary thermal decomposition studies of **6**, **7**, and **8** indicate that the complexes completely convert into the corresponding metaphosphates $M(PO_3)_2$ before 800 °C by the stepwise elimination of imidazole, isobutene, and water. However, there are some minor differences in the observed TGA and DTA behavior of the three complexes. The TGA data indicate that the onset temperature for the first weight loss varies over a range (see Supporting Information).

For example, the TGA and DTA studies on the cobalt derivative **6** reveal two distinct weight losses. The major weight loss (49%) occurs between 145 and 270 °C (endotherm at 227 °C in DTA) corresponding to the loss of four isobutene and two imidazole molecules. The second weight loss occurs gradually until 850 °C, corresponding to the loss of the remaining two imidazole molecules and the removal of two water molecules. The ceramic yield of 29% obtained at 850 °C exactly matches the theoretical yield for the formation of $Co(PO_3)_2$ material from **6**. No further weight loss is seen on heating the sample up to 1000 °C indicating no loss of P_2O_5 during the pyrolysis. A independent pyrolysis of the bulk sample of **6** which was heated for 6 h at 820 °C contained only one crystalline component (XRD), which has been reported as an unindexed phase with the stoichiometry $Co(PO_3)_2$.

The TGA and DTA studies of the Ni-derivative **7** shows a very similar behavior as that of **6**. It shows a two stage weight loss scheme for this compound; while the first weight loss is abrupt occurring between 200 and 270 °C, the second weight loss is much slower and is extended up to approximately 800

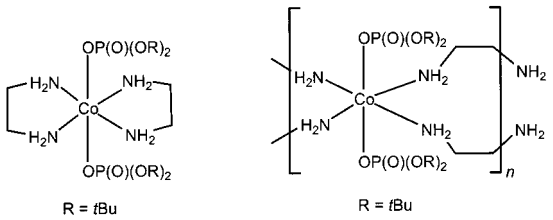

Figure 5. Possible molecular structures for $[Co(dtbp)_2(en)_2]$ (**9**).

°C. As in the case of **6**, the observed ceramic yield of the nickel metaphosphate $Ni(PO_3)_2$ at 800 °C is 29% exactly matching the expected theoretical yield of 28.9%.

There is a marked difference in the thermal behavior of the zinc derivative **8** compared to the cobalt and nickel derivatives **6** and **7** described above. First, the onset of the first weight loss is observed at as early as 132 °C. Second, the weight losses due to the removal of isobutene and imidazole molecules are well-resolved as evidenced by the two different sharp endotherms observed in the DTA of **8** at 144 and 222 °C, respectively. The loss of water molecules occur very slowly yielding the end ceramic product $Zn(PO_3)_2$ corresponding to 29.5% of the original material. (theoretical ceramic yield is 28.7%). Thermolysis of a bulk sample of **8** at 800 °C produced $Zn(PO_3)_2$ as the crystalline phase (by XRD). The elemental analysis of the ceramic materials obtained from **6**−**8** showed the presence of very small amounts carbon and hydrogen containing impurities (C analysis 0.47% for **6**; N analysis 0.47% for **6**; the nature of these impurities could not be established) probably due to the incomplete combustion of the imidazole molecules or nitride formation.

Ethylenediamine as Auxiliary Ligand. To assess the role of a neutral bidentate amine as auxiliary ligand, the above reactions were carried out using ethylenediamine (en) instead of imidazole. Thus, a 1:2 stoichiometric reaction between $Co(OAc)_2$ and dtbp-H in the presence of a slight excess of ethylenediamine in methanol at room temperature yields a yellowish orange product which analyzes to be $[Co(dtbp)_2(en)_2]$ (**9**) in a good yield. The IR spectrum of the complex exhibits a band at 1071 cm^{-1} assignable to the ν(P−O−M). The strong absorption at 1189 cm^{-1} is indicative of the presence of free phosphoryl P═O groups which are probably involved in some hydrogen bonding with ethylenediamine N−H protons. The broad band appearing around 3100−3400 cm^{-1} is due to the symmetric and antisymmetric stretching frequency of the NH_2 group of the en ligand. The solid-state DR visible spectra of the complex exhibits a band at 21 370 cm^{-1} assignable to (ν_3) $^4T_{1g}(F) \rightarrow {}^4T_{1g}(P)$ transition in Co(II) complexes having an octahedral arrangement.

Due to persistent twinning problems in the crystals of **9**, we were not able to obtain X-ray structure of this compound. However, based on the analytical data and IR and visible spectral measurements, it is clear that the cobalt atom is in an octahedral environment coordinated by four nitrogen atoms (of the two ethylenediamine ligands) and two oxygen atoms (of the two dtbp ligands) as shown in Figure 5. Either a discrete mononuclear or a polymeric structure is possible for this formulation. At the present time, in the absence of a single-crystal X-ray diffraction study, it is not possible to choose between these two structures in the solid state. Further, other modes of coordination of the en ligand (such as one intra and two intermolecular bridges per metal, or a random combination of all types; not shown in Figure 10) cannot be ruled out for the structure of **9**.

3,5-Dimethylpyrazole as Auxiliary Ligand. To study the effect of substituted/bulkier amines in these reactions, we carried

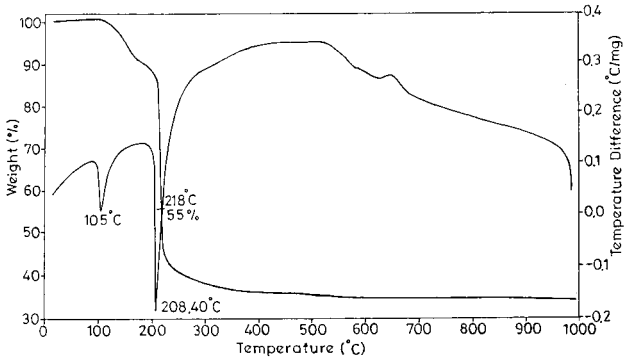

Figure 6. TGA and DTA traces of $[Co(dtbp)_2(3,5\text{-}dmp)_2]$ (**10**).

Scheme 3

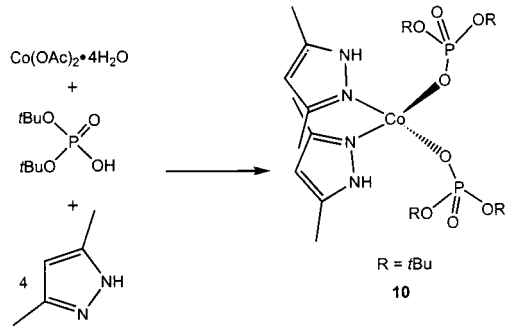

out a reaction between cobalt acetate and dtbp-H in the presence of a slight excess of 3,5-dimethylpyrazole as the auxiliary ligand to obtain $[Co(dtbp)_2(3,5\text{-}dmp)_2]$ (**10**) as the only cobalt containing product (Scheme 3). Thus, the use of a bulkier amine has changed the geometrical preference of Co^{2+} ion from an octahedral to tetrahedral[30] coordination environment. Analytically pure **10**, obtained by recrystallization from toluene, was characterized with the aid IR and visible spectroscopic studies, thermal analyses, and single-crystal X-ray diffraction studies. Unlike the other phosphate molecules described vide supra, compound **10** is highly soluble in most organic solvents including aliphatic and aromatic hydrocarbons. The UV−vis spectrum of **10** in methanol shows two absorption maxima at 16 640 and 17 450 cm^{-1} corresponding to (ν_3) $^4A_{2g}(F) \rightarrow {}^4T_{1g}(P)$ transitions of the tetrahedral Co(II) complex.[27]

Thermal Studies on 10. As in the case of both imidazole and ethylenediamine bound metal phosphate molecules, compound **10** also shows a clean conversion to the cobalt metaphosphate material under thermolysis conditions (Figure 6). The TGA and DTA studies on **10** testify to this fact. The TGA curve shows a two stage abrupt weight loss corresponding to a 67% reduction in the total mass of the sample between 100 and 310 °C. The DTA trace also shows two sharp endotherms at 105 and 208 °C corresponding to the successive loss of isobutene and 3,5-dmp molecules. The small and very slow 2% weight loss observed between 340 and 600 °C corresponds to the loss of two molecules of water per molecule of **10** to result in a ceramic material corresponding to the 34.1% of the total weight of the sample. The theoretical yield for the formation of $Co(PO_3)_2$ from **10** is 32.4%. The slightly higher percentage of the ceramic material obtained is probably due to the presence of some impurities along with the metaphosphate.

(30) Co^{2+} forms more tetrahedral complexes than any other transition metal ion due to a very small CFSE difference between the Oh and Td coordination environments (loss is only 0.27 Δ_o for a weak ligand field).

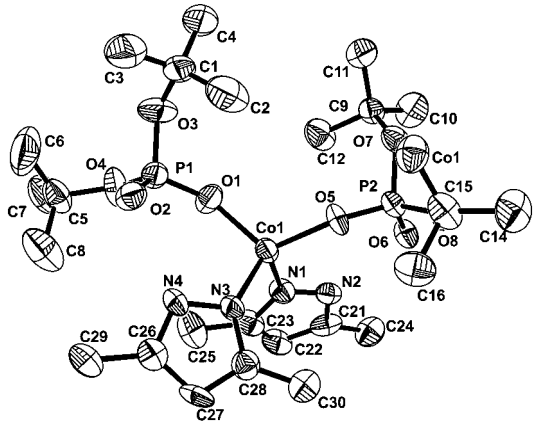

Figure 7. Thermal ellipsoid plot of $[Co(dtbp)_2(3,5\text{-}dmp)_2]$ (**10**) at 50% probability level.

Table 3. Selected Bond Lengths (Å) and Angles (deg) for **10**

Co(1)−O(5)	1.922(5)	Co(1)−O(1)	1.929(5)
Co(1)−N(1)	2.018(7)	Co(1)−N(3)	2.029(7)
P(1)−O(2)	1.490(6)	P(1)−O(1)	1.496(6)
P(1)−O(3)	1.561(7)	P(1)−O(4)	1.571(7)
P(2)−O(6)	1.491(6)	P(2)−O(5)	1.509(6)
P(2)−O(7)	1.581(6)	P(2)−O(8)	1.588(6)
O(7)−C(9)	1.471(10)	O(8)−C(13)	1.475(10)
O(4)−C(5)	1.454(12)	O(3)−C(1)	1.481(13)
N(2)−N(1)	1.347(9)	N(4)−N(3)	1.354(9)
O(5)−Co(1)−O(1)	116.0(3)	O(5)−Co(1)−N(1)	107.5(3)
O(1)−Co(1)−N(1)	108.2(3)	O(5)−Co(1)−N(3)	112.7(3)
O(1)−Co(1)−N(3)	106.0(3)	N(1)−Co(1)−N(3)	105.9(3)
O(2)−P(1)−O(1)	116.2(3)	O(2)−P(1)−O(3)	111.6(4)
O(1)−P(1)−O(3)	109.8(4)	O(2)−P(1)−O(4)	113.1(4)
O(1)−P(1)−O(4)	103.9(4)	O(3)−P(1)−O(4)	100.9(4)
O(6)−P(2)−O(5)	116.1(3)	O(6)−P(2)−O(7)	112.2(3)
O(5)−P(2)−O(7)	108.8(3)	O(6)−P(2)−O(8)	108.2(3)
O(5)−P(2)−O(8)	109.1(3)	O(7)−P(2)−O(8)	101.4(3)
P(2)−O(5)−Co(1)	140.1(4)	C(9)−O(7)−P(2)	127.1(6)
C(13)−O(8)−P(2)	128.0(6)	P(1)−O(1)−Co(1)	141.7(4)
C(5)−O(4)−P(1)	129.7(6)	C(1)−O(3)−P(1)	127.9(6)

Crystal Structure of 10. To clearly establish the solid-state structure of **10**, a single-crystal X-ray study was performed. A perspective view of the thermal ellipsoid plot of **10** with atom labeling scheme is shown in Figure 7. Selected bond lengths and angles are listed in Table 3. The molecule is made up of a Co^{2+} cation coordinated by two anionic phosphate ligands ($(t\text{-}BuO)_2PO_2^-$) and two neutral 3,5-dmp ligands. The L−Co−L angles (105.9(3)−116.0(3)°) in the molecule are indicative of a slightly distorted tetrahedral geometry. Similarly, the angles around the two phosphorus atoms in the molecule also deviate considerably from the ideal tetrahedral values (101.4(3)−116.2(3)°). The two Co−O distances are nearly equal (av 1.926 Å) and are slightly lower than the Co−O distance observed for the octahedral phosphate complex described above. The P═O distances are only marginally shorter (av 1.490 Å) than the P−O(Co) distances (av 1.502 Å), while the P−O(C) distances are considerably longer (av 1.575 Å). In contrast to the structure of the octahedral complex **6**, there are no hydrogen bonds formed in **10** between the N−H groups of the 3,5-dmp ligand and the free phosphoryl P═O groups. This difference could probably be ascribed to the presence of bulky $-CH_3$ group around the N−H group of the 3,5-dmp ligand.

Conclusion

In this contribution, we have presented a new synthetic methodology for the preparation of molecular divalent transition metal phosphates which undergo facile low-temperature thermolysis to afford corresponding metal−phosphate ceramic materials. This synthetic strategy has several advantages over the earlier methods described in the literature for the preparation of metal di-*tert*-butyl phosphate complexes, which include: (a) the use of cheaper and commercially available metal acetates as starting materials, (b) the use of less stringent reaction conditions without employing any anaerobic conditions, and (c) the use of water or methanol as reaction medium. It has also been demonstrated that, while the product of the direct reaction between metal acetate and dtbp-H yields a mixture of phosphates on thermolysis, the use of auxiliary ligands yields mononuclear products which yield only one type of ceramic material on thermolysis at higher temperatures. Further it has been shown that by fine-tuning the steric bulkiness of the auxiliary ligand used, it is possible to change the coordination environment around the metal as in the case of **10**.

Thermolysis of the molecular precursors reveal that the complexes **4** and **5** decompose cleanly to eliminate isobutene gas at 170 and 93 °C, respectively, while the gas evolution temperatures are slightly increased (to around 200 °C) for complexes **6**−**10**. However, in all cases, the removal of all organic moieties is over before 400 °C, after which only condensation reaction takes place to remove the hydrogen content as water molecules.

The approach to molecular precursors described by us in this paper appears to be more general and we are presently in the process of extending this chemistry for the preparation of other transition metal and main group metal phosphates.[31]

Experimental Section

Instruments and Methods. Since most of the starting materials and the products were found to be stable toward moisture and air, *no specific precautions were taken* to rigorously exclude air, although all manipulations were routinely carried out on a vacuum line. Elemental analyses were performed on a Carlo Eraba (Italy) Model 1106 Elemental Analyzer at IIT-Bombay. The melting points were measured in glass capillaries. Mass spectra were obtained on a Finnigan MAT 8330 system and a Varian MAT CH5 mass spectrometer. Powder XRD measurements were obtained on a PW1729 X-ray generator. The IR and NMR spectral measurements, and TGA and DTA studies were carried out as described previously.[32]

Solvents and Starting Materials. Commercial grade solvents were purified by employing conventional procedures and were distilled prior to their use. Starting materials such as $Co(OAc)_2{\cdot}4H_2O$ (Fluka), $Ni(OAc)_2{\cdot}4H_2O$ (Belami & Co), $Zn(OAc)_2{\cdot}2H_2O$, and imidazole (OFC, Bombay) were procured from commercial sources and used as received; 3,5-dimethylpyrazole was synthesized by previously reported method.[33] Di-*tert*-butyl phosph*ate* (dtbp-H) was synthesized from di-*tert*-butyl phosph*ite* using a previously reported procedure.[17] Due to its thermal instability, dtbp-H was freshly prepared from its potassium salt prior to its use.

Synthesis of $[Co_4(\mu_4\text{-}O)(dtbp)_6]$ (4). A hot solution of $Co(OAc)_2{\cdot}4H_2O$ (620 mg, 2.5 mmol) in MeOH (25 mL) was directly added to a THF solution (10 mL) of dtbp-H (790 mg, 3.75 mmol) and the mixture was stirred for ∼12 h at room temperature. The crude product was obtained by removing the solvent in a vacuum. Analytically pure product was obtained as deep-blue fiberlike crystals (875 mg) by leaving the reaction mixture for over 2 d on the benchtop. Several attempts to re-crystallize the sample in a variety of solvents in order to obtain X-ray

(31) Our preliminary results suggest the formation of interesting polyhedral cages and polymeric structures for Cu(II), Mn(II), Mn(III), and Ba(II) ions.

(32) Murugavel, R.; Karambelkar, V. V.; Anantharaman, G.; Walawalkar, M. G. *Inorg. Chem.* **2000**, *39*, 1381.

(33) Vogel's *Text Book of Practical Organic Chemistry*, 5th ed.; Langman Group: Essex, Harlow, U.K., 1989; Chapter 8, Exp. 8.14.

Table 4. Crystal Data and Experimental Details for the Structure Determination of **6**, **8**, and **10**

	6	**8**	**10**
empirical formula	$C_{28}H_{52}CoN_8O_8P_2$	$C_{28}H_{52}N_8O_8P_2Zn$	$C_{26}H_{52}CoN_4O_8P_2$
fw	749.65	756.09	669.59
temp	293(2)	293(2)	293(2)
wavelength	0.71073	0.71073	0.71073
cryst syst	triclinic	triclinic	tetragonal
space group	$P\bar{1}$	$P\bar{1}$	$P4_1$
a, Å	8.525(1)	8.488(1)	18.114(1)
b, Å	9.331(3)	9.333(1)	18.114(1)
c, Å	12.697(2)	12.723(2)	10.862(1)
α, deg	86.40(2)	86.55(1)	
β, deg	88.12(3)	88.04(1)	
γ, deg	67.12(2)	67.42(1)	
vol, Å^3; *Z*	928.6(4); 1	928.9(3); 1	3564.0(4); 4
density (calcd), g cm^{-3}	1.341	1.352	1.248
μ, mm^{-1}	0.603	0.802	0.617
R_1, R_{w2} [$I > 2\sigma(I)$][a]	0.0635; 0.1377	0.0519; 0.1297	0.0503; 0.1152
R_1, R_{w2} (all data)[a]	0.1484; 0.1569	0.0633; 0.1352	0.1195; 0.1280

[a] $R_1 = ||F_o| - |F_c||/|F_o|$; $R_{w2} = \{[w(F_o^2 - F_c^2)^2]/[w(F_o^2)^2]\}^{1/2}$.

quality crystals were unsuccessful. Characterization data for **4** and other compounds are listed in Table 1. IR (KBr): 2979(vs), 2936(m), 1578(m), 1487(m), 1400(m), 1368(s), 1251(vs), 1183(vs), 1078(vs), 1003(vs), 926(m), 842(m), 715(s), 550(m), 511(m) cm^{-1}. Diffuse Reflectance UV−vis: 15 530 and 19 920 cm^{-1}. MS (EI, 70 eV): *m*/*z* 1506 (M^+).

Synthesis of [Zn$_4$(μ_4-O)(dtbp)$_6$] (5). To a solution of $Zn(OAc)_2 \cdot 2H_2O$ (548 mg, 2.5 mmol) dissolved in hot THF (25 mL), a solution of dtbp-H (787 mg, 3.75 mmol) in THF (10 mL) was directly added under stirring. Compound **5** separated as an insoluble white solid from the reaction mixture after five minutes of the addition. The stirring was continued for an additional 12 h to ensure the completion of the reaction. The white solid thus obtained (794 mg (83%); lit.[14] 61% starting from $ZnMe_2$) was separated by filtration and dried in air for 24 h.

Synthesis of [M(dtbp)$_2$(imz)$_4$] (M = Co(6); Ni (7); Zn (8)). A solution of $M(OAc)_2 \cdot xH_2O$ (0.5 mmol) in MeOH (25 mL) was added into a solution of dtbp-H (210 mg, 1 mmol) in MeOH (10 mL) with constant stirring and to the resulting solution in a small beaker, a solution of imidazole (136 mg, 2 mmol) in THF (5 mL) was added slowly along the walls and left for crystallization. Crystalline products **6**−**8** (317 mg of **6**; 321 mg of **7**, 266 mg of **8**) were obtained after a few days. IR data (KBr) for **6**: 3118(s), 3052(s), 2973(s), 2940(s), 2875(s), 2723(w), 2631(w), 1460(w), 1368(m), 1256(w), 1216(vs), 1071(vs), 985(vs), 834(s), 755(s), 729(s), 663(s), 591(s), 512(s) cm^{-1}. **7**: 3115(s), 3046(s), 2976(m), 2936(s), 2877(s), 2720(s), 2632(w), 1546(w), 1500(w), 1459(m), 1390(m), 1362(s), 1257(s), 1213(vs), 1070(vs), 976(vs), 882(w), 832(s), 748(s), 719(s), 668(s), 625(s), 590(s), 552(s), 496(s) cm^{-1}. IR data (KBr) for **8**: 3108(s), 3045(s), 2982(s), 2933(s), 2870(s), 2713(m), 2626(m), 1456(m), 1372(m), 1251(w), 1211(vs), 1070(vs), 978(vs), 833(s), 758(s), 723(m), 661(m), 589(m), 561(m), 495(s) cm^{-1}. ^{1}H NMR for **8** ($CDCl_3$, 300 MHz, external standard $SiMe_4$): δ 1.3(s, C(CH_3), 36H), 7.04(s, CH, 8H), 7.7(s, CH, 4H).

Synthesis of [Co(dtbp)$_2$(en)$_2$] (9). A solution of $Co(OAc)_2 \cdot 4H_2O$ (59 mg, 0.23 mmol) in MeOH (15 mL) was added into a solution of dtbp-H (100 mg, 0.5 mmol) in MeOH (10 mL) with constant stirring. After 10 min, a slight excess of ethylenediamine (0.1 mL) was added and left for crystallization. Slow evaporation of the reaction mixture yielded orange colored crystals of **9** (100 mg) after 2 weeks. IR (KBr): 3170(s), 2979(s), 1472(w), 1391(s), 1366(s), 1262(w), 1189(vs), 1071(vs), 979(vs), 919(w), 834(s), 729(m), 590(m), 558(w), 499(w) cm^{-1}.

Synthesis of [Co(dtbp)$_2$(3,5-dmp)$_2$] (10). A solution of $Co(OAc)_2 \cdot 4H_2O$ (44 mg, 0.18 mmol) in MeOH (25 mL) was added into a solution of dtbp-H (74 mg, 0.35 mmol) in MeOH (10 mL) and stirred for 2 h. A solution of 3,5-dimethylpyrazole (34 mg, 0.35 mmol) in THF (5 mL) was added to the above mixture and stirred for another 2 h. The resulting deep-blue color solution was left as such for crystallization. After 2 weeks a deep blue oil was obtained. This oil was dissolved in excess of toluene and left for crystallization at 5 °C. After 2 months blue colored crystals of **10** (93 mg) were obtained. IR (KBr): 3137(w) 2992(s) 2932(m) 2875(s), 2710(w), 2521(w), 1604(w), 1510(w), 1394(m), 1371(s), 1317(s), 1258(s), 1182(vs), 1086(vs), 1051(vs), 977(vs), 830(s), 790(s), 749(s), 699(s), 612(s), 512(s), 468(s) cm^{-1}.

X-ray Structure Analysis. Single crystals of **6**, **8**, and **10** suitable X-ray structure analysis were grown using the procedures described vide supra. Cell determination and Intensity data collection were carried out on a Nonius MACH-3 Diffractometer at room temperature (293 K). In each case, unit cell dimensions were determined using 25 well-centered and well-separated strong reflections. The resultant intensity data were corrected for Lorentz and polarization effect but not for absorption effects. Structures were solved using direct methods (SHELXS-96)[34a] and refined using SHELXL-97.[34b] The positions of hydrogen atoms were geometrically fixed and were refined using a riding model. All non-hydrogen atoms were refined anisotropically. Other details pertaining to data collection, structure solution, and refinement are given in Table 4. Atomic coordinates, complete bond distances and bond angles, and anisotropic thermal parameters of all non-hydrogen atoms for all three compounds are deposited as Supporting Information.

Acknowledgment. Generous financial support by DST, New Delhi (SP/S1/F19/98), for carrying out this work and also the purchase of a MBraun Glovebox is gratefully acknowledged. This work was also supported by a DAE Young Scientist Research Award to R.M. The authors thank the DST funded Single Crystal X-ray Diffractometer Facility at IIT-Bombay for the X-ray Diffraction data, and the RSIC, IIT-Bombay, for the TGA and DTA measurements. We are grateful to Dr. R. Gopi Chandran for useful discussions during various stages of this work.

Supporting Information Available: X-ray data (including experimental details, atomic coordinates, complete bond lengths and angles, anisotropic thermal parameters, and hydrogen atom coordinates for compounds **6**, **8** and **10** (Tables S1−S15). EIMS of **4**, DR UV spectra of **4**, **6**, **9**, and **10**, and TGA DTA traces of **5**−**8** (Figures S1−S4). This material is available free of charge via the Internet at http://pubs.acs.org.

IC0006100

(34) (a) Sheldrick, G. M. *SHELXS-93: Program for Crystal Structure Solution*; University of Göttingen: Göttingen, Germany, 1993. (b) Sheldrick, G. M. *SHELXL-97: Program for Crystal Structure Refinement*; University of Göttingen: Göttingen, Germany, 1997.